

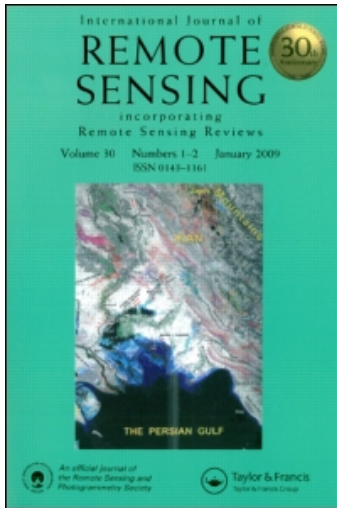
This article was downloaded by: [George Mason University]

On: 7 October 2010

Access details: Access Details: [subscription number 915935488]

Publisher Taylor & Francis

Informa Ltd Registered in England and Wales Registered Number: 1072954 Registered office: Mortimer House, 37-41 Mortimer Street, London W1T 3JH, UK



International Journal of Remote Sensing

Publication details, including instructions for authors and subscription information:

<http://www.informaworld.com/smpp/title~content=t713722504>

Identification of ocean oil spills in SAR imagery based on fuzzy logic algorithm

Peng Liu^a; Chaofang Zhao^a; Xiaofeng Li^b; Mingxia He^a; William Pichel^c

^a Ocean Remote Sensing Institute, Ocean University of China, Key Laboratory for Ocean Remote Sensing, Ministry of Education of China, Qingdao, China ^b IMIS at NOAA/NESDIS, NOAA E/RA3, WWBG, Camp Springs, MD, USA ^c NOAA/NESDIS/STAR, NOAA E/RA3, WWBG, Camp Springs, MD, USA

Online publication date: 28 September 2010

To cite this Article Liu, Peng , Zhao, Chaofang , Li, Xiaofeng , He, Mingxia and Pichel, William(2010) 'Identification of ocean oil spills in SAR imagery based on fuzzy logic algorithm', International Journal of Remote Sensing, 31: 17, 4819 – 4833

To link to this Article: DOI: 10.1080/01431161.2010.485147

URL: <http://dx.doi.org/10.1080/01431161.2010.485147>

PLEASE SCROLL DOWN FOR ARTICLE

Full terms and conditions of use: <http://www.informaworld.com/terms-and-conditions-of-access.pdf>

This article may be used for research, teaching and private study purposes. Any substantial or systematic reproduction, re-distribution, re-selling, loan or sub-licensing, systematic supply or distribution in any form to anyone is expressly forbidden.

The publisher does not give any warranty express or implied or make any representation that the contents will be complete or accurate or up to date. The accuracy of any instructions, formulae and drug doses should be independently verified with primary sources. The publisher shall not be liable for any loss, actions, claims, proceedings, demand or costs or damages whatsoever or howsoever caused arising directly or indirectly in connection with or arising out of the use of this material.

Identification of ocean oil spills in SAR imagery based on fuzzy logic algorithm

PENG LIU*[†], CHAOFANG ZHAO[†], XIAOFENG LI[‡], MINGXIA HE[†]
and WILLIAM PICHEL[§]

[†]Ocean Remote Sensing Institute, Ocean University of China, Key Laboratory for
Ocean Remote Sensing, Ministry of Education of China, Qingdao, 266100, China

[‡]IMSG at NOAA/NESDIS, NOAA E/RA3, WWBG, Camp Springs,
MD 20746-4304, USA

[§]NOAA/NESDIS/STAR, NOAA E/RA3, WWBG, Camp Springs,
MD 20746-4304, USA

Ocean oil spills cause serious damage to the marine environment, especially around coastal waters. Synthetic aperture radar (SAR) has been proven to be a useful tool for oil spill detection under low to moderate wind conditions. SAR operates in the microwave band and the data is not affected by the cloud cover and day/night conditions. However, the operational application of SAR for oil spill detection in the ocean is limited by false alarm targets or lookalike phenomena such as low wind speed, natural films, etc. In this study, we develop analysis of variance (ANOVA) to extract the features based on their characteristic geometry, grey level and texture features in the SAR images. We further analysed a fuzzy logic algorithm to separate oil spills features from lookalikes. We trained this algorithm using 38 SAR images (11 ENVISAT-Advanced Synthetic Aperture Radar (ASAR) and 27 European Remote Sensing (ERS)-2 SAR images) with 120 known oil spills and 80 lookalikes to generate an oil spill probability of a dark pixel in a SAR image. An independent set of 26 SAR images were used to validate the algorithm and it was found that 80.9% of the oil spills were correctly classified, and 20.0% of the lookalikes were wrongly classified as oil spills. The complete algorithmic procedure was coded in Matlab7.0 using its Fuzzy Logic Toolbox.

1. Introduction

The marine environment is an important subject of public concern as marine transport trade increases and marine petroleum resources have been developed at the present time. Oil spills frequently occur in the ocean environment. It is important to detect oil spills in a timely manner and to take effective measures to protect the marine environment. In recent years, remote sensing instruments have become one of the main methods in marine oil spill detection. Among which, synthetic aperture radar (SAR) can provide high resolution images with wide area coverage, day and night, and all-weather capabilities.

Generally, the radar's return comes from the interaction between the radar beam and capillary and short ocean gravity waves, i.e. sea surface roughness of about the same wavelength as that of the radar wave. Oil on the sea surface is observed on SAR images as dark areas because the viscoelastic property of oil slicks dampens the short-wave field due to both suppression of wave growth and increase of wave dissipation (Alpers and Huhnerfuss 1988) which reduces the radar backscattering from the sea

*Corresponding author. Email: liupeng-qdst@163.com

surface. However, not all dark features on the ocean surface are oil spills. They could be lookalikes such as low wind areas, natural films, wind front areas, wind shadows near an island, rain cells, current shear zones, internal waves and upwelling zones. To effectively use SAR imagery for ocean oil spill detection, one must develop a set of rules to separate lookalikes from the actual oil spills.

In the literature, the two main methods of statistical-based and neural network based classification have been proposed for distinguishing oil spills from lookalikes. Solberg *et al.* (1999, 2003, 2007) detected oil slicks from SAR images by combining a statistical model with a rule-based approach. Prior knowledge such as the distance between the oil slicks and ships was incorporated into their model. Using European Remote Sensing Satellite (ERS) images, Del Frate *et al.* (2000) detected oil spills based on a multilayer perceptron (MLP) neural network. Topouzelis *et al.* (2008) presented an oil spill detection method with a radial basis function (RBF) neural network. Karantzas and Argialas (2008) used a geometric level set segmentation to detect possible oil spills and a classification was performed for the separation of lookalikes. All the above studies use either 'YES' or 'NO' to represent the oil slick or the lookalike. Generally, improving the accuracy of detection will increase the false alarm rate (FAR), and vice versa.

Apart from the above-mentioned two methods, Keramitsoglou *et al.* (2006) recently set up a fuzzy logic system to give the probability of oil spills by using nine images for training and 26 images for testing. In their system, the selected input variables consisted of five geometry parameters including the total number of dark objects identified in the image, the area of the candidate dark object, the eccentricity of the object's shape, the proximity of the object to land, and the number of dark objects in the vicinity of a candidate dark object. The system analysed the five parameters of the samples and assigned the probability of a dark pattern to be an oil spill. It shows a higher detection accuracy and a lower FAR over other methods.

In this study, we fine-tuned a fuzzy logic system based on the special features of oil spills in the China Seas with a training set of 38 SAR images. A one-way analysis of variance (ANOVA) was used to select the effective feature variables. These variables were then combined with geometry features, the backscatter level and texture features as input variables to fuzzy logic system (Topouzelis *et al.* 2008) to generate a better oil spill detection approach.

The paper is organized in four sections. Section 2 describes the dataset and methodology. Results and conclusions follow in §3 and §4, respectively.

2. Dataset description and methodology

2.1 Dataset description

In this study, full-resolution ERS-2 SAR and ENVISAT-Advanced Synthetic Aperture Radar (ASAR) images were obtained from the European Space Agency (ESA) under the framework of the Dragon project. ERS-2 SAR images of the precision image (PRI) product have a pixel size of $12.5 \text{ m} \times 12.5 \text{ m}$ with a swath width of 100 km. ENVISAT-ASAR images include the Image Mode (IM) and Wide Swath Mode (WSM) products. The IM product is similar to the PRI product of the ERS-2 SAR, while the WSM product has a spatial resolution of 150 m with a swath width of 450 km.

All SAR images were acquired in the China seas (Bohai Sea, Yellow Sea, East China Sea and South China Sea) between 1995 and 2007. Each selected SAR image contains a certain number of dark spots corresponding to oil spills or lookalikes on

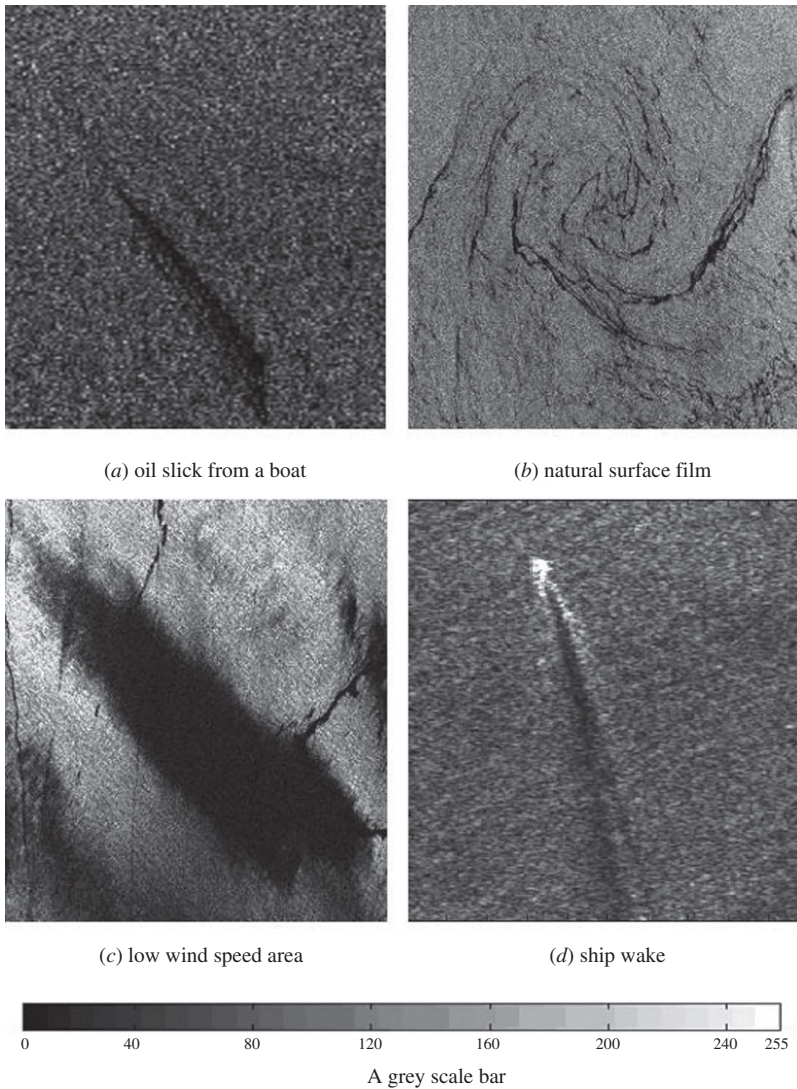


Figure 1. Four examples of SAR images that contain dark features.

the sea surface. These SAR images were used to establish the fuzzy logic system, in which 38 SAR images (11 ENVISAT-ASAR and 27 ERS-2 SAR images) were used for training and a set of independent 26 test images were used to validate the algorithm. Figure 1 shows the examples of oil spills and lookalikes such as natural surface film, low wind speed area and ship wakes, respectively.

Information for confirmed oil spills comes from three data sources: (1) the ‘tropical and subtropical ocean viewed by ERS SAR’ project, which provides the known oil spills in SAR images (<http://www.ifm.zmaw.de/fileadmin/files/ers-sar/index.html>); (2) the published papers, which provide well known oil spill accidents in SAR images (Yu *et al.* 2007, Shi *et al.* 2008); (3) the results from the experts’ intuition and experience (Brekke and Solberg 2005).

In general, oil slicks can be classified in four main categories based on characteristics of the shape of dark patches: (1) thin, line-type slick which might be caused by a ship or a stationary object, such as an oil platform with a small amount of oil released; (2) wide, regular slicks caused by a stationary object with a larger amount of oil released; (3) wide, irregular slicks caused by wind and/or current influence; (4) thin, piecewise line-type slicks caused by a moving ship changing directions, or a thin slick altered by wind or current (Brekke and Solberg 2005).

2.2 Methodology

All SAR images are calibrated including compensation of the attenuation due to the incidence angle variation, geo-referenced, and mapped. A 3×3 Lee filter is applied to original image, followed by a 5×5 Lee filter and a 7×7 Median filter. This combination has been previously used with success for speckle removal for SAR (Karathanassi *et al.* 2006).

Automatic oil spill detection in SAR images was implemented by a series of computational procedures including calibration and filtering, segmentation, feature extraction and classification.

2.2.1 Image segmentation. After image filtering, the next processing step was image segmentation. To this end, a combination of OTSU (Otsu 1979) and Max-entropy method was used to determine the appropriate threshold that would constrain the segmentation. OTSU is an implementation of the OTSU threshold technique. The histogram is divided into two classes. The threshold is determined by minimizing the inter-class variance and maximizing the outer-class variance of the image. Suppose the grey value of the image is varied from 0 to T , the grey value t_1 is recorded as the threshold for image segmentation when the variance of the inter-class reaches its minimum and the variance of the outer-class reaches its maximum. Max-entropy is another threshold technique. The maximum value of entropy occurs at the junction of the object and the sea background. When the sum of local entropy of the object area and background reaches the maximum, the grey value t_2 is recorded for the threshold of image segmentation. In this study, we set the threshold to t_1 if t_1 was less than the average grey value of the whole image; otherwise, we set the threshold to t_2 . Finally the segmented image was processed by a 7×7 median filter because there were still many small black noise spots after the segmentation.

Figure 2 shows the oil pollution accident that occurred in Bohai Bay in March 2006. The No. 2 oil spill object shown in figure 2 was estimated to be about 103.3 km^2 by the combination of OTSU and Max-entropy methods, which is similar to the actual value of 119.95 km^2 given by Yu *et al.* (2007).

2.2.2 Feature extraction. From the threshold dark spot image, feature extraction was carried out for each slick. Table 1 summarizes 18 features of the slick used in the literature (Del Frate 2000, Assilzadeh and Mansor 2001):

- (a) *Geometry and shape of the segmented region:* the complexity (COM), a ratio between the square of the perimeter and the area of an object and form factor (FF), a ratio between the width and length of an object (Gasull *et al.* 2002) was used in this paper.
- (b) *Physical characteristics of the backscatter level of the spot and its surroundings:* we used two parameters: (1) a ratio between average backscattering and its standard deviation outside the area (RBSDO) (Nirchio *et al.* 2005); (2) a mean

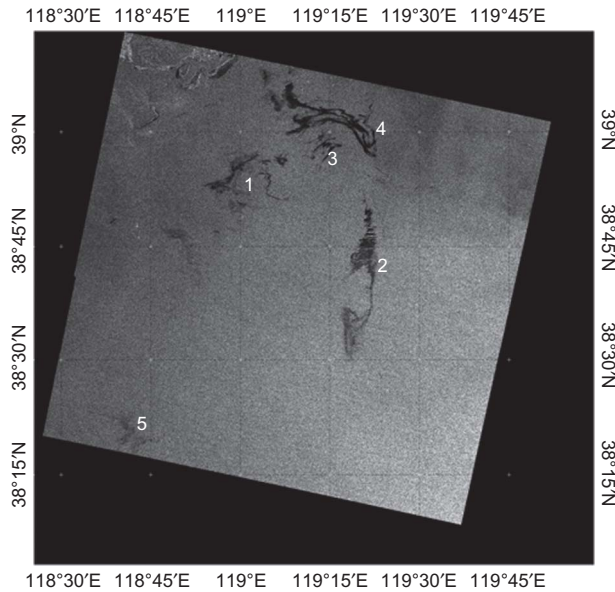


Figure 2. The oil pollution accident that occurred in March 2006 in Bohai Bay.

Table 1. The ANOVA result for feature variable selection (five features shown in bold face with p -value less than 0.005).

No.	Feature	p -value	No.	Feature	p -value	No.	Feature	p -value
1	COM	E-6	7	Mean contrast (3/4)	0.07	13	Second-order moment	0.23
2	FF	E-8	8	SD ratio of object and background	0.29	14	Third-order moment	0.35
3	Object area average	0.23	9	Ratio 3–5	0.84	15	Fourth-order moment	0.40
4	Background average	0.45	10	RBSDO	0.04	16	Entropy	0.51
5	Object standard deviation	0.19	11	Ratio 9–10	0.15	17	ASM	0.03
6	Gradient	0.68	12	Bounding box average	0.06	18	ESO	E-4

contrast (between object and background), which is easily affected by wind speed and is generally high for oil spills (Del Frate *et al.* 2000).

- (c) *Texture features*: texture features provide information on the structural arrangement of pixels and their spatial correlation among surrounding pixels. Assilzadeh and Mansor (2001) described an early warning system for oil spills with texture features based on a grey level co-occurrence matrix (GLCM). The

texture features provide information about the relative position of various grey levels within the image. The GLCM estimated the number of pairs of adjacent pixels $p(i, j, d, \theta)$ (here i, j are the location of pixel; and d, θ are the distance and direction for one pair of pixels). In this study, we calculated the image entropy in different directions corresponding to direction θ of $0^\circ, 45^\circ, 90^\circ$ and 135° . The value of entropy for each pixel was calculated in a $7^\circ \times 7^\circ$ window based on the GLCM with a displacement of $d (d^\circ = 1)$. The final entropy was an average of all the four directions. Generally, $p(i, j, d, \theta)$ was written as $p(i, j)$ in brief. Based on the GLCM, Haralick *et al.* (1973) suggested 14 statistical parameters (shown in table 1) to describe texture features. Two significant parameters, angular second moment (ASM) and entropy second order (ESO) were used in our system, where ASM was calculated as:

$$\text{ASM} = \sum_{i=0}^M \sum_{j=0}^M p(i, j). \quad (1)$$

ESO was calculated as:

$$\text{ESO} = - \sum_{i=0}^M \sum_{j=0}^M p(i, j) \times \lg p(i, j) \quad (2)$$

ASM is the measure of the smoothness of the image. The smoother the region, the less uniformly $p(i, j)$ is distributed and the higher is ASM. ESO is a measure of disorder of the image in a local window along a certain orientation with a certain displacement. ESO represents the measure of randomness and takes low value for smooth images.

2.2.3 Features classification. Actually many features have been used to distinguish the oil spill and the lookalikes (Topouzelis *et al.* 2008). In order to establish the fuzzy logic system, the features should be selected based on the complexity of fuzzy rule-based systems and our datasets for oil spill and the lookalikes. If the number of features increase and the fuzzy values are not at ordinal scales, the complexity of rule-based generation will increase manyfold. Therefore, the selected feature should exhibit a strong relationship between the value of the selected feature and the probability of it being an oil spill. In this case, the fuzzy rule base could be established according to the statistical analysis of each selected feature.

A one-way ANOVA was used to evaluate the importance of the various features in distinguishing oil spills from the lookalikes (Topouzelis *et al.* 2008). ANOVA was used to test the differences among two or more independent groups. The smaller the probability of the F distribution, the more important the variable is. Table 1 shows the results of ANOVA variables for all 18 features. It is common to declare a variable significant if the probability value (p -value) is less than 0.05 (Hogg and Ledolter 1987).

As the probability of a dark spot on the SAR image to be an oil spill is a function of many factors, it is very important to select the key parameters from different features listed in table 1. The selection of the input variables should be considered with respect to two aspects: the first is that the most important features should be included; and the second one is that the fuzzy logic system remains a reasonable size. Based on the above criteria and ANOVA test, we found five important parameters including: COM, FF, RBSDO, ASM and ESO, shown in table 1 in boldface.

2.2.4 Identification of oil spills based on fuzzy logic system

(1) Introduction of the fuzzy logic algorithm

Fuzzy logic theory, introduced by Zadeh in 1965, simulates the way that people make inferences and decisions (Zadeh 1965). Information flowing in the fuzzy model requires that the input variables go through three major processes known as fuzzification, fuzzy inference, and defuzzification (Zhao and Li 2007). These three processes are shown in figure 3 and briefly summarized here:

1. Fuzzification: in this process, input variables of the system are decomposed into one or more fuzzy sets; therefore, a number of fuzzy perceptions of the input are produced.
2. Fuzzy inference: after the inputs have been decomposed into fuzzy sets, a set of fuzzy if-then-else rules are used to process the inputs and produce a fuzzy output. Each rule consists of one condition and one action, and the condition is interpreted from the input fuzzy set.
3. Defuzzification: in this process, the output is estimated from the output fuzzy set. The output is the result of the weighted mean from all the individual fuzzy rules in the fuzzy logic model

In this study, we used the most popular fuzzy model, the Mamdani fuzzy model.

(2) Development of the training set

Fuzzy sets are defined for all input variables. The range of input variables is chosen based on the histogram of the test dataset. Here, we use variable RBSDO (definition refers to the feature extraction in §2.2.2) as an example. Figure 4 shows the histogram of variable RBSDO. The fuzzy set defined for the input variable RBSDO is given in figure 5. There are three RBSDO peaks between intervals [2.0, 4.0], [4.0, 6.4] and [6.4, 10.3]. Corresponding probabilities of oil spill are about 30%, 53% and 75%, respectively. Therefore, three fuzzy sets namely ‘Small’, ‘Medium’, and ‘Big’ are defined on the input space for RBSDO. The bigger the RBSDO value, the more likely the object is an oil spill. The statistical relationship between RBSDO and the probability of dark objects to be oil spills in figure 6 shows that the fuzzy memberships could be converted into three ordinal classes during the development of rule base.

Similarly, we can define ‘Small’, ‘Medium’, and ‘Big’ fuzzy sets for variables COM, FF, ASM and ESO (definition refers to the feature extraction in §2.2.2), respectively. Based on the training dataset, we find that the ranges of these variables are $COM \in$

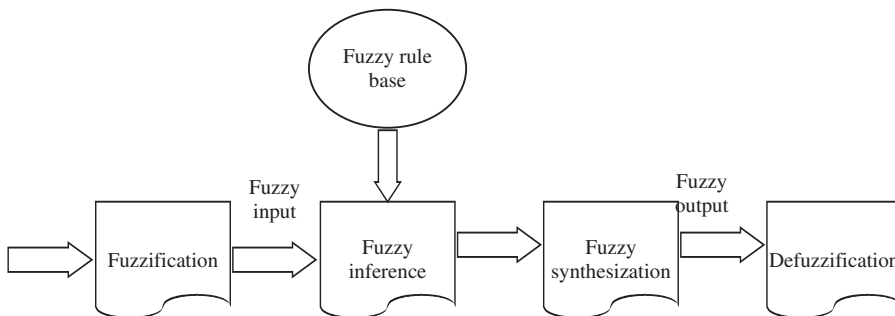


Figure 3. The main framework of fuzzy logic.

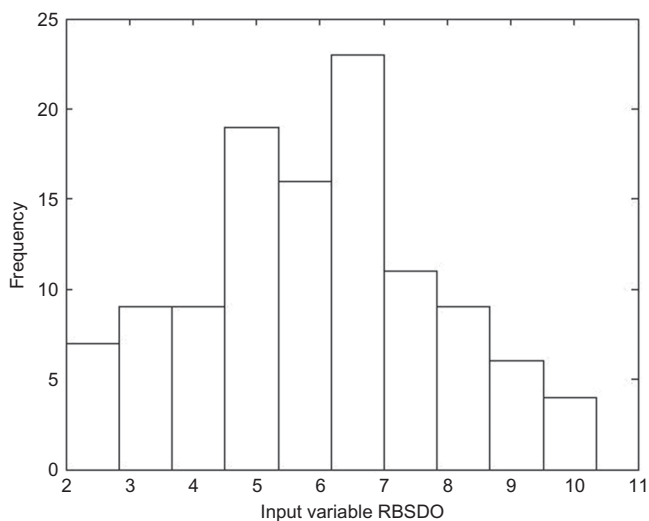


Figure 4. The histogram of RBSDO. RBSDO is a ratio between average backscattering and its standard deviation outside the area (Nirchio *et al.* 2005). Its unit is null.

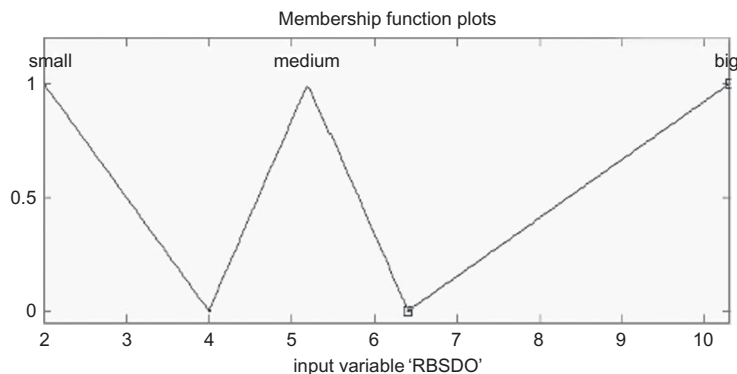


Figure 5. The fuzzy set of variable RBSDO.

[3.6, 2460], $FF \in [0.02, 0.86]$, $ASM \in [2.2 \times 10^{-4}, 380 \times 10^{-4}]$, and $ESO \in [6.0, 13.0]$. The bigger the COM, FF and ASM, the less likely the observed object is an oil spill. The bigger the ESO, the more likely the observed object is an oil spill.

For the output variable ‘probability of an object to be an oil spill’, we defined two fuzzy sets covering [0,1] domain (corresponding to 0–100%). For this output variable, two triangular fuzzy sets were defined in output space.

(3) Development of the rule base

A number of fuzzy rules were developed and trained based on the 38 SAR images in the China Seas. Each image contains up to 10 potential oil slicks. The total training and validation dataset has about 120 known oil spills and 80 lookalikes.

In our fuzzy logic system, 243 rules were created by the permutation and combination of three fuzzy sets from five variables, RBSDO, COM, FF, ASM and ESO. Each

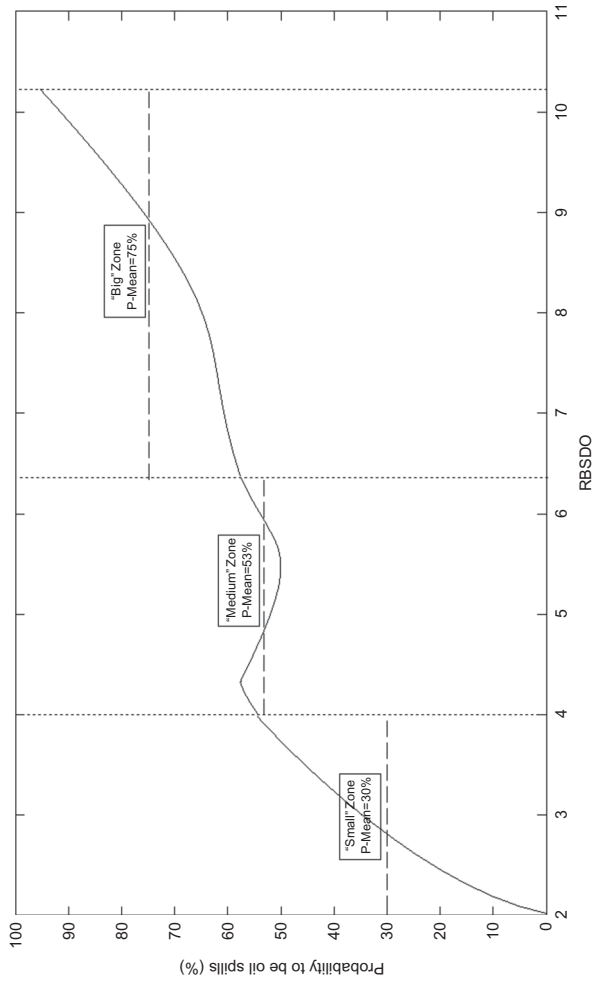


Figure 6. Statistics of regularity between RBSDO and probability of dark objects to be oil spills.

fuzzy rule was a combination of the input variables. All the rules were used by the logical AND operation. An example of these fuzzy rules is shown as:

'If the variable COM is small **AND** the variable FF is small **AND** the variable RBSDO of the dark object is big **AND** the variable ASM is small **AND** the variable ESO is big **THEN** the probability of the candidate dark spot to be an oil spill is **HIGH**.'

In order to generate the probability estimation of the candidate dark object to be an oil spill, figure 3 shows the flow chart of the fuzzification–inference–defuzzification processes:

- Fuzzification: this process is used to determine the degree of truth for each rule, where the triangular functions are defined for each input variable.
- Inference: during the inference process, we define the assignment of the output fuzzy set for each rule. In this study, the min–max inference technique was used. The combined fuzzy output function was constructed by combining the results of all the fuzzy rules. If an output fuzzy set was activated by more than one rule, the maximum of all activations was chosen in the output function.
- Defuzzification: the final output of the fuzzy system is the probability of the object to be an oil spill. Therefore the fuzzy output needs to be defuzzified. The centroid defuzzification method is used to estimate the crisp value of the output variable by finding the centre of area below the combined membership function.

The implementation of the fuzzification, rule-inference, and defuzzification of the algorithm was based on numerical analysis approximation of the problem. More specifically, the area covered within the participation functions as calculated by rules was computed as a definite integral using a Simpson's rule (Atkinson 1989).

3. Results

The fuzzy logic system was developed and trained with 38 SAR images. An independent 26 test SAR images were used to validate the results. Among them, 21 images contain confirmed oil spills and five contain confirmed lookalikes. Analysis shows that 17 oil-spill images and four lookalikes images were classified correctly.

Two additional case studies are carried out in the China seas.

3.1 Case 1

An oil accident occurred off the west coast of Sabah (Borneo) in the South China. Figure 7 shows an ERS-2 SAR image acquired over the South China Sea at 02:27 (UTC) on 13 July 1997. The image presents a large number of dark spots. The dark areas, marked as objects 1 and 2 in the left part of the image, were caused by oil discharged from the ship. The ship (white spot) is visible at the front of the oil trail (object 2) and the dark streaky features (object 3 and 4) visible in the right part of the image originate from natural oil seeps (<http://www.ifm.zmaw.de/fileadmin/files/ers-sar/Sdata/oceanic/oilpol/singa/116523483ERS2.html>). Table 2 shows the fuzzy logic result of the probability to be an oil spill (P) for each dark spot. The algorithm depicted correctly the verified oil-spill objects 1 and 2, and assigned to each of them a high probability of 81.2%. The algorithm also depicted the verified lookalike objects

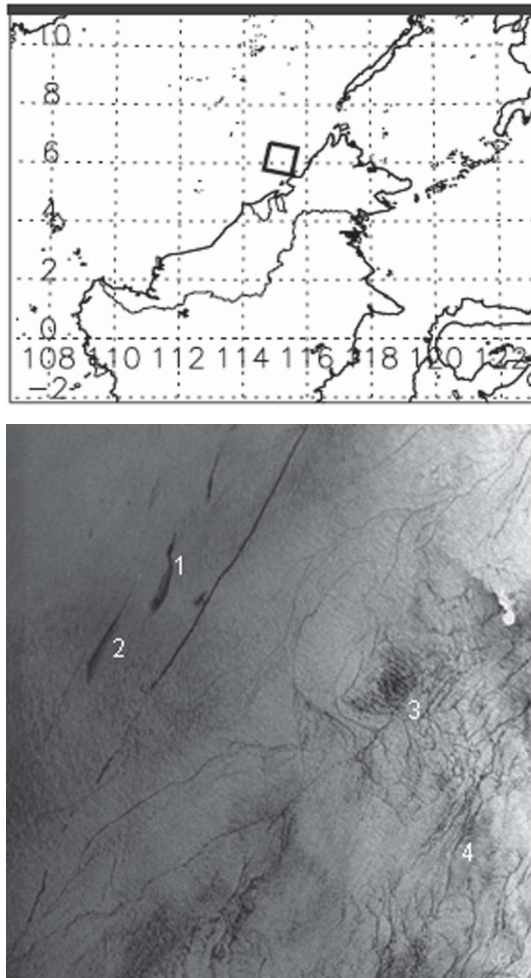




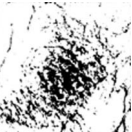

Figure 7. ERS-2 SAR image acquired on 13 July 1997 at 02:27 UTC (image centre at $6^{\circ} 07' N$, $115^{\circ} 12' E$). Objects 1 and 2 were oil spills caused by oil discharged from ships, and objects 3 and 4 were lookalikes.

3 and 4, and assigned each of them a low probability of 21.8% and 24.9%, respectively. One can see that the lookalikes can be easily rejected using a threshold.

3.2 Case 2

Figure 8 shows an ERS-1 SAR image acquired over the Yellow Sea taken at 02:31 (Coordinated Universal Time, UTC) on 19 June 1995. The image presents a larger number of dark regions compared with the first case study. Only object 9 is a lookalike phenomenon caused by natural oil seeps; the others are oil spills caused by leaking from nearby oil platforms (<http://www.ifm.zmaw.de/fileadmin/files/ers-sar/Sdata/>

Table 2. Results of the probability to be oil spills of the dark spots in figure 7. (P stands for the probability to be an oil spill.).

Object no.	Dark spot	COM	FF	RBSDO	ASM ($\times 10^{-4}$)	EOS	P (%)
1		77.00	0.10	5.78	3.33	12.26	81.2
2		87.53	0.13	5.74	2.73	12.41	81.2
3		1284.90	0.26	4.71	13.2	10.00	21.8
4		479.82	0.29	3.06	27.6	11.34	24.9

oceanic/oilpol/yellowsea/2053 22889ERS1.html). Table 3 shows the fuzzy logic results for the objects 1–9. One can see that the dark object 9 has low probability to be an oil spill but the others have high probability. The algorithm depicted both the verified oil spills (objects 1–8) and the lookalike (object 9) correctly.

4. Conclusion

A system for the identification of possible oil spills has been developed based on a fuzzy logic algorithm. In this system, SAR images were calibrated, geo-referenced, mapped, filtered and processed so that the appropriate dark spots were extracted to estimate the necessary feature variables. Eighteen feature characteristics, which include geometry, grey level and texture features, were calculated and evaluated by ANOVA to determine whether the dark features were oil spills or lookalikes. We find that only five features including RBSDO, COM, FF, ASM and ESO were needed to separate oil spills from lookalikes as the input variables for the fuzzy logic system. In our fuzzy logic system, 243 rules were created by the permutation and combination of the five features' three fuzzy sets. The fuzzy logic system was trained with 38 SAR images and then validated using an independent 26 images in the China Seas. Candidate oil spill objects were fuzzy classified to determine the probability of each individual object to be an oil spill. The resulting images and tables were provided with the probability of oil spill and other relevant information for supporting decision making. Analysis of 26 SAR images show that 80.9% of the oil spills were correctly

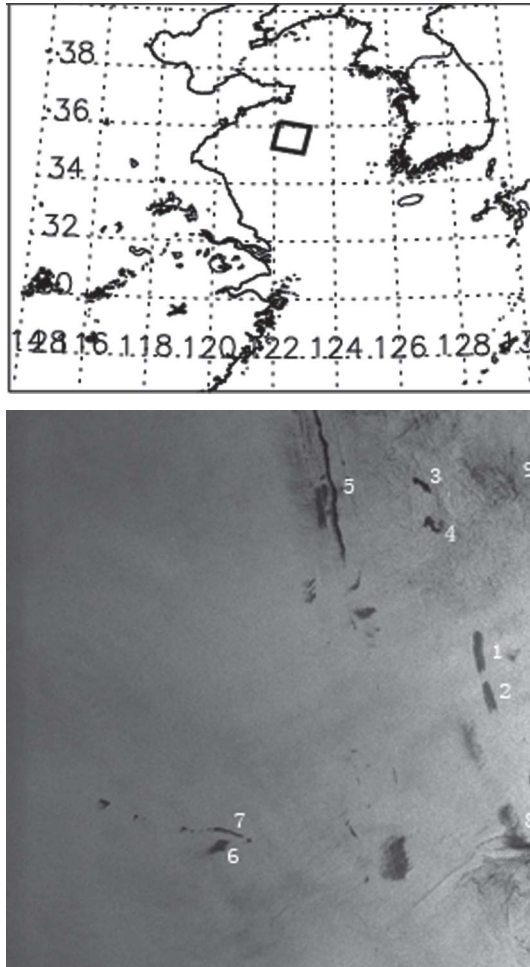











Figure 8. ERS-1 SAR image acquired on 19 June 1995 at 02:31 UTC (image centre at 35°37' N, 122°35' E). Object 9 was the lookalike phenomenon; the others were oil spills caused by oil platforms.

classified, and 20.0% of the lookalikes were wrongly classified as oil spills. The system can be adopted to use in other geographical areas as well. The time required for the whole process (from preprocessing to fuzzy classification) is on the order of 5–6 min per dark spot on a regular personal computer.

Our study shows that the five selected features, including geometry, grey level and texture features, are important to separate oil spills from lookalikes. There are still other features that could be considered. For example, geographical information such as the distance from the centre of a dark spot to a boat, environmental information such as the wind speed of the scene (Espedal and Wahl 1999), or polarization features such as entropy, mean scatter angle and anisotropy (Migliaccio and Gambardella 2007) could all be considered to enhance the oil spill detection capability of the fuzzy logic system.

Table 3. Results of the probability to be oil spills of the dark spots in figure 8. (P stands for the probability to be an oil spill.).

Object no.	Dark spot	COM	FF	RBSDO	ASM ($\times 10^{-4}$)	EOS	P (%)
1		37.42	0.09	6.57	4.70	11.95	71.1
2		49.43	0.12	5.63	6.25	11.98	74.5
3		9.20	0.07	6.07	7.66	11.87	63.6
4		24.67	0.10	5.89	3.70	12.29	81.2
5		121.76	0.08	5.25	4.36	11.82	57.7
6		21.14	0.10	5.06	4.39	12.13	81.2
7		13.73	0.10	6.42	3.74	12.18	82.1
8		35.82	0.08	4.75	4.40	11.89	63.9
9		2184.1	0.4	6.73	4.28	11.87	25.0

Acknowledgements

SAR images were provided by ESA through ESA-NRSCC Dragon Cooperation Program, project 2566 and the ESA AO Envisat project 226, 431 and 6133. The views, opinions, and findings contained in this report are those of the authors and should not be construed as an official NOAA or US Government position, policy, or decision.

References

- ALPERS, W. and HUHNERFUSS, H., 1988, Radar signatures of oil films floating on the sea surface and marangoni effect. *Journal of Geophysical Research*, **93**, pp. 3642–3648.
- ASSILZADEH, H. and MANSOR, S.B., 2001, Early warning system for oil spill using SAR images. In *Proceedings of the ACRS 2001–22nd Asian Conference on Remote Sensing*, 5–9 November 2001, Singapore, vol. 1 pp. 460–465.
- ATKINSON, A., 1989, *An Introduction to Numerical Analysis*, 2nd edn (Chichester: John Wiley & Sons).
- BREKKE, C. and SOLBERG, A.H.S., 2005, Oil spill detection by satellite remote sensing. *Remote Sensing of Environment*, **95**, pp. 1–13.

- DEL FRATE, F., PETROCCHI, A., LICHTENEGGER, J. and CALABRESI, G., 2000, Neural networks for oil spill detection using ERS-SAR data. *IEEE Transactions on Geoscience and Remote Sensing*, **38**, pp. 2282–2287.
- ESPEDAL, H.A. and WAHL, T., 1999, Satellite SAR oil spill detection using wind history information. *International Journal of Remote Sensing*, **20**, pp. 49–65.
- GASULL, A., FABREGAS, X., JIMENEZ, J., MARQUES, F., MORENO, V. and HERRERO, M., 2002, September. Oil spills detection in SAR images using mathematical morphology. In *Proceedings of the European Signal Processing Conference 2002*, Toulouse, France, vol. 1, pp. 25–28.
- HARALICK R.H., 1972, Fourier preprocessing for hand print character recognition. *IEEE Transactions on Computers*, **21**, pp. 195–201.
- HARALICK, R.H., SHANUMUGAM, K. and DINSTEN, I., 1973, Textual features for image classification. *IEEE Transactions on Systems, Man and Cybernetics*, **SMC-3**, pp. 610–621.
- HOGG, R.V. and LEDOLTER, J., 1987, *Engineering Statistics* (New York: MacMillan).
- KARANTZALOS, K. and ARGIALAS, D. 2008. Automatic detection and tracking of oil spills with level set segmentation from SAR imagery. *International Journal of Remote Sensing*, **29**, pp. 6281–6296.
- KARATHANASSI, V., TOPOUZELIS, K., PAVLAKIS, P. and ROKOS, D., 2006, An object-oriented methodology to detect oil spills. *International Journal of Remote Sensing*, **27**, pp. 5235–5251.
- KERAMITSOGLU, I., CARTALIS, C. and KIRANOUDIS, C., 2006, Automatic identification of oil spills on satellite images. *Environmental Modelling and Software*, **21**, pp. 640–652.
- MIGLIACCIO, M. and GAMBARDILLA, A., 2007, SAR polarimetry to observe oil spills. *IEEE Transactions on Geoscience and Remote Sensing*, **45**, pp. 506–511.
- NIRCHIO, F., SORAGENT, M., GIANCASPRO, A., BIAMINO, W., PARISATO, E., RAVERA, R. and TRIVERO, R., 2005, Automatic detection of oil spills from SAR images. *International Journal of Remote Sensing*, **26**, pp. 1157–1174.
- SHI, L., IVANOV, A., HE, M. and ZHAO, C., 2008, Oil spill mapping in the Yellow Sea and East China Sea using synthetic aperture radar imagery. *International Journal of Remote Sensing*, **29**, pp. 6315–6329.
- OTSU, N., 1979, A threshold selection method from gray-level histogram [J]. *IEEE Transactions on Systems, Man and Cybernetics*, **9**, pp. 62–66.
- SOLBERG, A.H.S., BREKKE, C. and HUSØY, P.O., 2007, Oil spill detection in Radarsat and Envisat SAR images. *IEEE Transactions on Geoscience and Remote Sensing*, **45**, pp. 746–755.
- SOLBERG, A.H.S., DOKKEN, S.T. and SOLBERG, R., 2003, Automatic detection of oil spills in Envisat, Radarsat and ERS SAR images. In *Proceedings of IEEE International Geoscience and Remote Sensing Symposium, 2003*, Toulouse, France, vol. 4, pp. 2747–2749.
- SOLBERG, A.H.S., STORVIK, G., SOLBERG, R. and VOLDEN, E., 1999, Automatic detection of oil spills in ERS SAR images. *IEEE Transactions on Geoscience and Remote Sensing*, **37**, pp. 1916–1924.
- TOPOUZELIS, K., KARATHANASSI, V., PAVLAKIS, P. and ROKOS, D., 2008, Dark formation detection using neural networks. *International Journal of Remote Sensing*, **29**, pp. 4705–4720.
- YU, W., LI, J., SHAO, Y., QI, X. and LIU, Y., 2007, Remote sensing techniques for oil spill monitoring in offshore oil and gas exploration and exploitation activities: case study in Bohai Bay. *Petroleum Exploration and Development*, **34**, pp. 378–383.
- ZADEH, L.A., 1965, Fuzzy sets. *Information and Control*, **8**, pp. 338–353.
- ZHAO, Q. and LI, Y., 2007, Monitoring marine oil-spill using microwave remote sensing technology. In *IEEE International Conference on Electronic Measurement and Instruments*, Xi'an, China, pp. 69–72.